Natural-convection boundary-layer flow on a vertical surface with Newtonian heating

J. H. Merkin
Department of Applied Mathematics, University of Leeds, Leeds, UK

The natural-convection boundary-layer flow on a vertical surface generated by Newtonian heating in which the heat transfer from the surface is proportional to the local surface temperature is discussed. Solutions valid near the leading edge and valid far downstream are obtained and are joined by a numerical solution of the governing equations. The solution far downstream gives rise to a novel similarity system that is analyzed in detail, with solutions being obtained for large and small values of the Prandtl number.

Keywords: natural convection boundary layers; Newtonian heat transfer

1. Introduction

The usual way in which natural convection flows are modeled is to assume that the flow is driven either by a prescribed surface temperature or by a prescribed surface heat flux. A large number of calculations have been performed, especially for the large Grashof number (or boundary-layer) limit, for such surface conditions and for various geometrical configurations. Much of this work is detailed in the recent book by Gebhart et al. (1988). Here a somewhat different driving mechanism for the natural-convection boundary-layer flow is considered in that it is assumed that the flow is set up by Newtonian heating from the bounding surface. In particular, the heat transfer from the surface is taken to be proportional to the local surface temperature.

A situation somewhat similar to that treated here arises in what are usually termed conjugate convective flows, where the heat is supplied to the convecting fluid through a bounding surface with a finite heat capacity. This results in the heat transfer rate through the surface being proportional to the local difference in temperature with the ambient conditions (see, for example, Pop et al. 1985; Pozzi and Lupo 1988; Merkin and Pop 1993). This configuration has also arisen in a model of the convective flow set up when the bounding surface absorbs heat by solar radiation (Fathalah and Elsayed 1980). Merkin and Chaudhary (1994) have recently extended this work, in a model of convective flows driven by heat transfer from a catalytic surface reaction, to the case where the surface heat transfer is proportional to a general power of the temperature difference.

The flow on a vertical surface is considered, and a solution is sought by obtaining series expansions for stream function and temperature that are valid near the leading edge and far downstream. These two solution regions are then joined by a numerical solution of the full governing equations. It is found that near the leading edge the flow is driven, at leading order, by a constant heat flux from the surface, and the higher-order terms are then perturbations on the standard uniform heat-flux solution. This is the same behavior seen in the conjugate convection problem.

When the behavior of the solution far downstream is considered, it is found that there is an essential difference between the present case and the conjugate convection problem. For the conjugate convection problem, the flow far downstream approaches the standard isothermal wall solution. However, for the present case, the flow far downstream gives rise to a new similarity solution, and one of the main purposes of this paper is to treat this similarity solution in some detail. Solutions to this problem are obtained that are valid for both small and large values of the Prandtl number. It is seen that for moderate values of the Prandtl number, which are typical of gases, the surface temperature is very sensitive to Prandtl number variations. The basic equations and their appropriate nondimensionalization are given first.

2. Equations of motion

Consider a semi-infinite vertical flat surface with coordinates $\bar{x}$ and $\bar{y}$ measuring distance along and normal to it, with corresponding velocity components $\bar{u}$ and $\bar{v}$. On making the Boussinesq approximation, the equations governing the boundary-layer flow are

$$\frac{\partial \bar{u}}{\partial \bar{x}} + \frac{\partial \bar{v}}{\partial \bar{y}} = 0 \tag{1a}$$

$$\bar{u}\frac{\partial \bar{u}}{\partial \bar{x}} + \bar{v}\frac{\partial \bar{u}}{\partial \bar{y}} = g\beta(T - T_0) + \nu\frac{\partial^2 \bar{u}}{\partial \bar{y}^2} \tag{1b}$$

$$\bar{u}\frac{\partial T}{\partial \bar{x}} + \bar{v}\frac{\partial T}{\partial \bar{y}} = \frac{\nu}{\sigma}\frac{\partial^2 T}{\partial \bar{y}^2} \tag{1c}$$

where σ is used for the Prandtl number. The boundary and initial conditions are

$$\bar{u} = 0, \quad \bar{v} = 0, \quad \text{on } \bar{y} = 0, \quad \bar{u} \to 0, \quad T \to T_0 \text{ as } \bar{y} \to \infty, \quad (\bar{x} > 0) \tag{2a}$$

$$\frac{\partial T}{\partial \bar{y}} = -h_s T \quad \text{on } \bar{y} = 0, \quad (\bar{x} > 0) \tag{2b}$$

$$\bar{u} = 0, \quad \bar{v} = 0, \quad T = T_0 \quad \text{at } \bar{x} = 0, \quad (\bar{y} > 0) \tag{2c}$$

Address reprint requests to Professor Merkin at the Department of Applied Mathematics, University of Leeds, Leeds LS2 9JT, UK.

Received 8 October 1993; accepted 30 April 1994

for some (constant) heat transfer coefficient h_s. Note that boundary condition in Equation 2b is different from those taken previously.

To begin making Equations 1 and 2 dimensionless, we first note that scales for the temperature difference or for the streamwise length do not arise naturally. However, there is a temperature scale, T_0, and a scaling h_s for $\bar{y}$. This leads to the variables

$$T - T_0 = T_0\theta,\ y = h_s\bar{y} \tag{3a}$$

A balancing of terms in Equations 2a and 2b then leads to a steamwise length scale $\ell = \dfrac{g\beta T_0}{\nu^2 h_s^4}$, which suggests

$$\bar{u} = (\nu\ell h_s^2)u,\ \bar{v} = (\nu h_s)v,\ x = \bar{x}/\ell \tag{3b}$$

Applying the transformation of Equation 3 to Equations 1 and 2 gives

$$\frac{\partial u}{\partial x} + \frac{\partial v}{\partial y} = 0 \tag{4a}$$

$$u\frac{\partial u}{\partial x} + v\frac{\partial u}{\partial y} = \theta + \frac{\partial^2 u}{\partial y^2} \tag{4b}$$

$$u\frac{\partial \theta}{\partial x} + v\frac{\partial \theta}{\partial y} = \frac{1}{\sigma}\frac{\partial^2 \theta}{\partial y^2} \tag{4c}$$

subject to the boundary conditions

$$u = 0,\quad v = 0,\quad \frac{\partial \theta}{\partial y} = -(\theta + 1) \text{ on } y = 0$$

$$u \to 0,\quad \theta \to 0 \quad \text{as } y \to \infty \tag{5}$$

3. Solution

3.1. Solution for small x

The flow develops initially by heat flux from the surface, which suggests the transformation

$$\psi = x^{4/5}F(x, \zeta),\quad \theta = x^{1/5}H(x, \zeta),\quad \zeta = y/x^{1/5} \tag{6}$$

to obtain a solution valid near the leading edge (where ψ is the stream function). Applying equation 6 to equations 4 and 5 gives

$$\frac{\partial^3 F}{\partial \zeta^3} + H + \frac{4}{5}F\frac{\partial^2 F}{\partial \zeta^2} - \frac{3}{5}\left(\frac{\partial F}{\partial \zeta}\right)^2 = x\left(\frac{\partial F}{\partial \zeta}\frac{\partial^2 F}{\partial \zeta \partial x} - \frac{\partial F}{\partial x}\frac{\partial^2 F}{\partial \zeta^2}\right) \tag{7a}$$

$$\frac{1}{\sigma}\frac{\partial^2 H}{\partial \zeta^2} + \frac{4}{5}F\frac{\partial H}{\partial \zeta} - \frac{1}{5}H\frac{\partial F}{\partial \zeta} = x\left(\frac{\partial F}{\partial \zeta}\frac{\partial H}{\partial x} - \frac{\partial F}{\partial x}\frac{\partial H}{\partial \zeta}\right) \tag{7b}$$

subject to the boundary conditions

$$F = 0,\quad \frac{\partial F}{\partial \zeta} = 0,\quad \frac{\partial H}{\partial \zeta} = -1 - x^{1/5}H \quad \text{on } \zeta = 0$$

$$\frac{\partial F}{\partial \zeta} \to 0,\quad H \to 0 \quad \text{as } \zeta \to \infty \tag{7c}$$

These boundary conditions suggest looking for a solution by expanding

$$F(x, \zeta) = F_0(\zeta) + x^{1/5}F_1(\zeta) + \cdots \tag{8}$$

$$H(x, \zeta) = H_0(\zeta) + x^{1/5}H_1(\zeta) + \cdots$$

The leading-order terms (F_0, H_0) are given by uniform heat-flux solution (Sparrow and Gregg 1956). The effect of the Newtonian heating boundary condition is felt at $O(x^{1/5})$ through the boundary condition $H_1'(0) = -H_0(0)$, where $H_0(0)$ is known from the leading-order problem. The solution of the resulting equations is straightforward, and for $\sigma = 1$, it is found that

$$\theta_s = x^{1/5}(1.8728 + 2.5980x^{1/5} + \cdots)$$

$$\tau_w = x^{2/5}(1.3774 + 1.3450x^{1/5} + \cdots) \tag{9}$$

where $\theta_s = \theta(x, 0)$ and $\tau_w = \left(\dfrac{\partial u}{\partial y}\right)_{y=0}$.

3.2. Solution for large x

Well downstream, the convective flow is driven by the Newtonian heating. This consideration, together with an examination of Equations 4 and 5, leads to the transformation

$$\psi = x\,f(x, y),\quad \theta = x\,h(x, y) \tag{10}$$

with y left untransformed, in order to obtain an asymptotic solution. Applying Equation 10 to Equations 4 and 5 gives

$$\frac{\partial^3 f}{\partial y^3} + h + f\frac{\partial^2 f}{\partial y^2} - \left(\frac{\partial f}{\partial y}\right)^2 = x\left(\frac{\partial f}{\partial y}\frac{\partial^2 f}{\partial x \partial y} - \frac{\partial f}{\partial x}\frac{\partial^2 f}{\partial y^2}\right) \tag{11a}$$

$$\frac{1}{\sigma}\frac{\partial^2 h}{\partial y^2} + f\frac{\partial h}{\partial y} - h\frac{\partial f}{\partial y} = x\left(\frac{\partial f}{\partial y}\frac{\partial h}{\partial x} - \frac{\partial f}{\partial x}\frac{\partial h}{\partial y}\right) \tag{11b}$$

subject to the boundary conditions

$$f = 0,\quad \frac{\partial f}{\partial y} = 0\quad \frac{\partial h}{\partial y} + h = -x^{-1} \quad \text{on } y = 0$$

$$\frac{\partial f}{\partial y} \to 0,\quad h \to 0 \quad \text{as } y \to \infty \tag{11c}$$

These boundary conditions suggest looking for a solution by expanding in inverse powers of x. The leading-order terms (f_0, h_0) in such an expansion satisfy

$$f_0''' + h_0 + f_0 f_0'' - f_0'^2 = 0 \tag{12a}$$

$$\frac{1}{\sigma}h_0'' + f_0 h_0' - f_0' h_0 = 0 \tag{12b}$$

subject to

$$f_0(0) = 0,\quad f_0'(0) = 0,\quad h_0'(0) + h_0(0) = 0$$

$$f_0'(\infty) = 0,\quad h_0(\infty) = 0 \tag{12c}$$

(primes denote differentiation with respect to y).

Notation

g	Acceleration due to gravity
h_s	Surface heat transfer coefficient
T	Fluid temperature
T_0	Temperature of ambient fluid (constant)
$u, \bar{u}$	Velocity component in streamwise direction
$v, \bar{v}$	Velocity component in transverse direction
$x, \bar{x}$	Coordinate along the surface
$y, \bar{y}$	Coordinate normal to the surface

Greek symbols

β	Coefficient of thermal expansion
θ	Dimensionless temperature difference
θ_s	Dimensionless surface temperature
ν	Kinematic viscosity
σ	Prandtl number
τ_w	Dimensionless skin friction
ψ	Stream function

The solution of Equations 12 will be discussed in detail below. The solution will arise, for example, as the similarity solution when the surface heating, $\left(\frac{\partial T}{\partial y}\right)_{y=0}$, is proportional to the surface temperature difference, $(T - T_0)_{y=0}$, i.e., when the dimensionless boundary condition to be applied on $y = 0$ is modified to

$$\frac{\partial \theta}{\partial y} = -\theta \tag{13}$$

The problem when the right-hand side of Equation 13 is replaced by θ^N, for a general exponent N, has been treated for values of the Prandtl number of 0(1) by Merkin and Chaudhary (1994).

The boundary condition of Equations 11c suggest that the next term in the asymptotic expansion should be of $0(x^{-1})$. However, the solution at this stage is indeterminate because of the leading-edge shift effect (Stewartson 1964), and the expansion has to be modified to (Stewartson 1957)

$$f(x, y) = f_0(y) + x^{-1}(\log x\phi_1(y) + f_1(y)) + \cdots$$
$$h(x, y) = h_0(y) + x^{-1}(\log xg_1(y) + h_1(y)) + \cdots \tag{14}$$

The leading-order terms (f_0, h_0) satisfy Equations 12, and the terms $(\phi_1(y), g_1(y))$ are the eigensolutions

$$\phi_1 = \alpha f_0, g_1 = \alpha h_0 \tag{15}$$

for an as yet undetermined constant α. Using Equation 15, the equations for (f_1, h_1) are

$$f_1''' + h_1 + f_0 f_1'' - f_0' f_1' = \alpha(f_0'^2 - f_0 f_0'') \tag{16a}$$

$$\frac{1}{\sigma} h_1'' + f_0 h_1' - h_0 f_1' = \alpha(h_0 f_0' - f_0 h_0') \tag{16b}$$

subject to

$$f_1(0) = 0, \quad f_1'(0) = 0, \quad h_1'(0) + h_1(0) = -1$$
$$f_1'(\infty) = 0, \quad h_1(\infty) = 0 \tag{16c}$$

To solve Equations 16 numerically, it is necessary to construct two complementary functions namely, (f_a, h_a) and (f_b, h_b), where $f_a''(0) = 1$, $h_a(0) = 0$, $h_a'(0) = 0$, and $f_b''(0) = 0$, $h_b(0) = 1$, $h_b'(0) = 0$, and also to construct two particular integrals, namely, (f_c, h_c), for which $\alpha = 1$ and homogeneous boundary conditions are taken, and (f_d, h_d), for which $\alpha = 0$ and the condition $h_d'(0) + h_d(0) = -1$ is applied. The full solution is then given by

$$f_1 = af_a + bf_a + \alpha f_c + f_d \tag{17}$$
$$h_1 = ah_a + bh_b + \alpha h_c + h_d$$

for constants a and b. Now, as $y \to \infty$,

$$h_i \to A_i, \ f_i' \sim -\frac{A_i}{C_0} y + B_i \qquad (i = a, b, c, d) \tag{18}$$

for constants A_i and B_i and where $C_0 = f_0(\infty)$. The outer boundary conditions then give the equations

$$aA_a + bA_b + \alpha A_c + A_d = 0 \tag{19}$$
$$aB_a + bB_b + \alpha B_c + B_d = 0$$

However, the existence of the eigensolutions (Equations 13) means that $A_aB_b - A_bB_a = 0$, and consequently Equations 19 have a solution only if a compatibility condition is satisfied, and it is this condition that determines α. After a little algebra, it is found that

$$\alpha = \frac{A_bB_d - A_dB_b}{A_cB_b - A_bB_c} \tag{20}$$

The numerical integrations then give, for $\sigma = 1$, $\alpha = 0.43464$. However, the solution at this order is not fully determined, since any multiple of eigensolutions in Equations 15 can be added to the solution at $0(x^{-1})$, which it appears cannot be found from integrated forms of Equation 4c.

Finally, for $\sigma = 1$,

$$\theta_s \sim 7.9738x + \cdots, \quad \tau_w \sim 3.5090x + \cdots \tag{21}$$

as $x \to \infty$.

3.3. Numerical solution

To obtain a numerical solution of Equations 4 and 5 that will hold for all x, starting at $x = 0$ and proceeding downstream until the asymptotic solution as given by Equation 12 is attained, the method of continuous transformations described by Hunt and Wilks (1981) for general boundary-layer calculations is used. This method requires the use of a composite transformation of variables that reflects the transformations of Equations 6 for small x and Equations 10 for large x. Here the transformation

$$\psi = x^{4/5}(1 + x)^{1/5}\bar{f}(x, \bar{\eta}), \theta = x^{1/5}(1 + x)^{4/5}\bar{h}(x, \bar{\eta}),$$
$$\bar{\eta} = \frac{y(1 + x)^{1/5}}{x^{1/5}} \tag{22}$$

is applied. Expansion 8 shows that the solution has a singularity in x-derivatives as $x \to 0$; to remove this, the further transformation $\xi = x^{1/5}$ is made, with the numerical solution then proceeding stepwise in the ξ-direction. The details of the method have been described fully elsewhere (Mahmood and Merkin 1988) and need not be repeated here.

To show that the solution does in fact proceed smoothly from one that is valid for small x to the asymptotic form given above, graphs of $\bar{f}_{\bar{\eta}\bar{\eta}}(\xi, 0)$ and $\bar{h}(\xi, 0)$ for $\sigma = 1$ are shown in Figure 1 (plotted against ξ). These start at the values at the leading edge (as given by Equations 9) and approach their corresponding values downstream (as given by Equations 21). It can also be seen from this figure that the numerical integration gives an overshoot in both $\bar{f}_{\bar{\eta}\bar{\eta}}(\xi, 0)$ and $\bar{h}(\xi, 0)$. However, this is an artifact of applying a transformation (Equations 22). No such behavior is seen in plots of θ_s and τ_w, which are shown in Figure 2 for $\sigma = 0.72$, $\sigma = 1.0$, and $\sigma = 10.0$ (now plotted against x). Figure 2 shows that the straight-line variation of both θ_s and τ_w with x, as suggested by Equation 21, is rapidly attained, and that there are considerable differences in surface temperature when the Prandtl number is changed

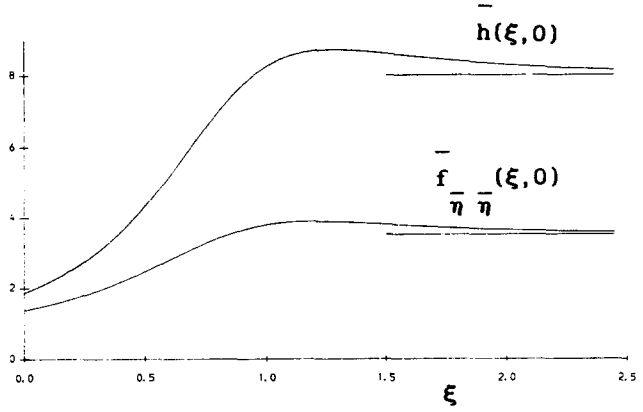

Figure 1 Graphs of $\bar{f}_{\bar{\eta}\bar{\eta}}(\xi, 0)$ and $\bar{h}(\xi, 0)$ plotted against $\xi = x^{1/5}$ for $\sigma = 1$, obtained from the numerical integration of Equations 4 and 5.

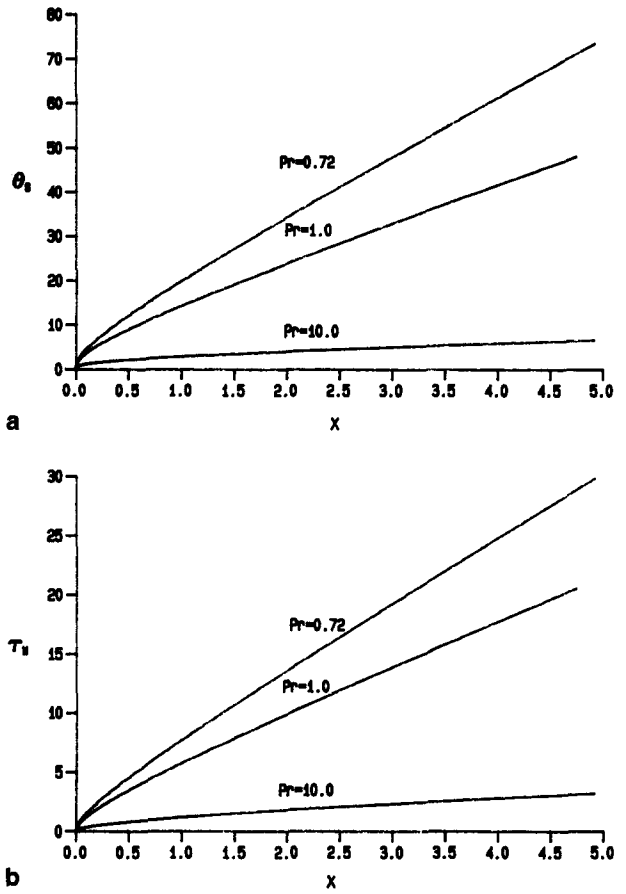

Figure 2 Graphs of (a) θ_s and (b) τ_w plotted against x for $\sigma = 0.72$, 1.0, and 10.0, obtained from the numerical integration of Equations 4 and 5.

by the relatively small amount from $\sigma = 1.0$ to $\sigma = 0.72$ (characteristic of air). This sensitivity of surface temperature to changes in the Prandtl number, at least for relatively small values of σ, is highlighted in Figure 3 where θ_s and τ_w are plotted against x for $\sigma = 0.1$ and 0.2. (Note the difference in scale between this figure and Figure 2.) Here it can clearly be seen that a change in $\sigma = 0.2$ from $\sigma = 0.1$ produces a very substantial change in θ_s. This point is now considered further by examining the solution of the similarity system (Equations 12) in more detail.

4. Similarity equations

In this section, the solution of Equations 12 is considered in more detail (dropping the suffix for convenience). In particular, solutions valid for both $\sigma \gg 1$ and $\sigma \ll 1$ are obtained. It has already been established in Merkin and Chaudhary (1994), for physically realistic solutions, i.e., those that have $h \geq 0, f' \geq 0$ on $0 \leq y < \infty$, that $h(y) > 0$ on $0 \leq y < \infty$ and that $h(y)$ is strictly monotone decreasing on this range.

The numerical solution of the boundary-value problem (Equations 12) is straightforward, and graphs of $f''(0)$ and $h(0)$ are shown in Figure 4 (in Figure 4a for $\sigma \geq 1$ and in Figure 4b for $\sigma \leq 1$). Figure 4 shows that both $f''(0)$ and $\theta(0)$ decrease as σ increases, whereas they both increase very rapidly as σ is decreased (note the considerable differences in scale between Figures 4a and 4b). This behavior is now examined in more detail.

4.1. Solution for $\sigma \gg 1$

A consideration of both the numerical results for large values of σ and Equations 12 suggests that the solution develops a two-region structure as $\sigma \to \infty$, namely, an inner region of O(1) thickness that is driven by the buoyancy force and a much thicker outer region in which the fluid is isothermal. A balancing of the terms in Equations 12 shows that the appropriate scalings for the inner region are

$$f = \sigma^{-1}\phi, \quad h = \sigma^{-1}g \tag{23}$$

leaving y unscaled. These transformations give

$$\phi''' + g + \sigma^{-1}(\phi\phi'' - \phi'^2) = 0 \tag{24a}$$

$$g'' + \phi g' - \phi' g = 0 \tag{24b}$$

subject to

$$\phi(0) = 0, \quad \phi'(0) = 0, \quad g'(0) = -g(0) \tag{24c}$$

with the outer boundary conditions relaxed at this stage.

Equation 24a suggests looking for a solution by expanding in inverse powers of σ. The leading-order terms (ϕ_0, g_0) satisfy the equations

$$\phi_0''' + g_0 = 0 \tag{25a}$$

$$g_0'' + \phi_0 g_0' - \phi_0' g_0 = 0 \tag{25b}$$

to be solved subject to Equations 24c, and outer conditions that

$$\phi_0'' \to 0, \; g_0 \to 0 \qquad \text{as } y \to \infty \tag{25c}$$

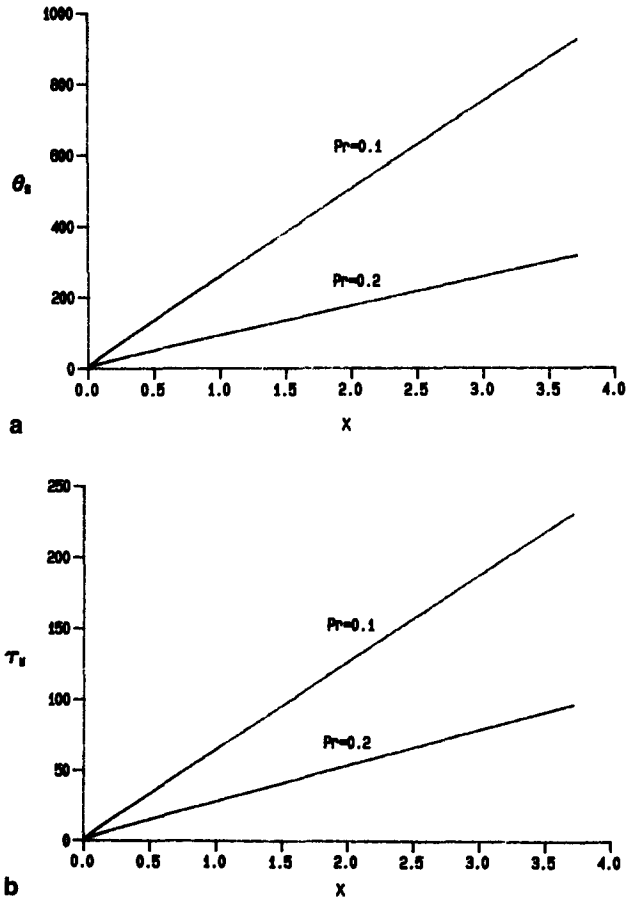

Figure 3 Graphs of (a) θ_s and (b) τ_w plotted against x for $\sigma = 0.1$ and $\sigma = 0.2$, obtained from the numerical integration of Equations 4 and 5.

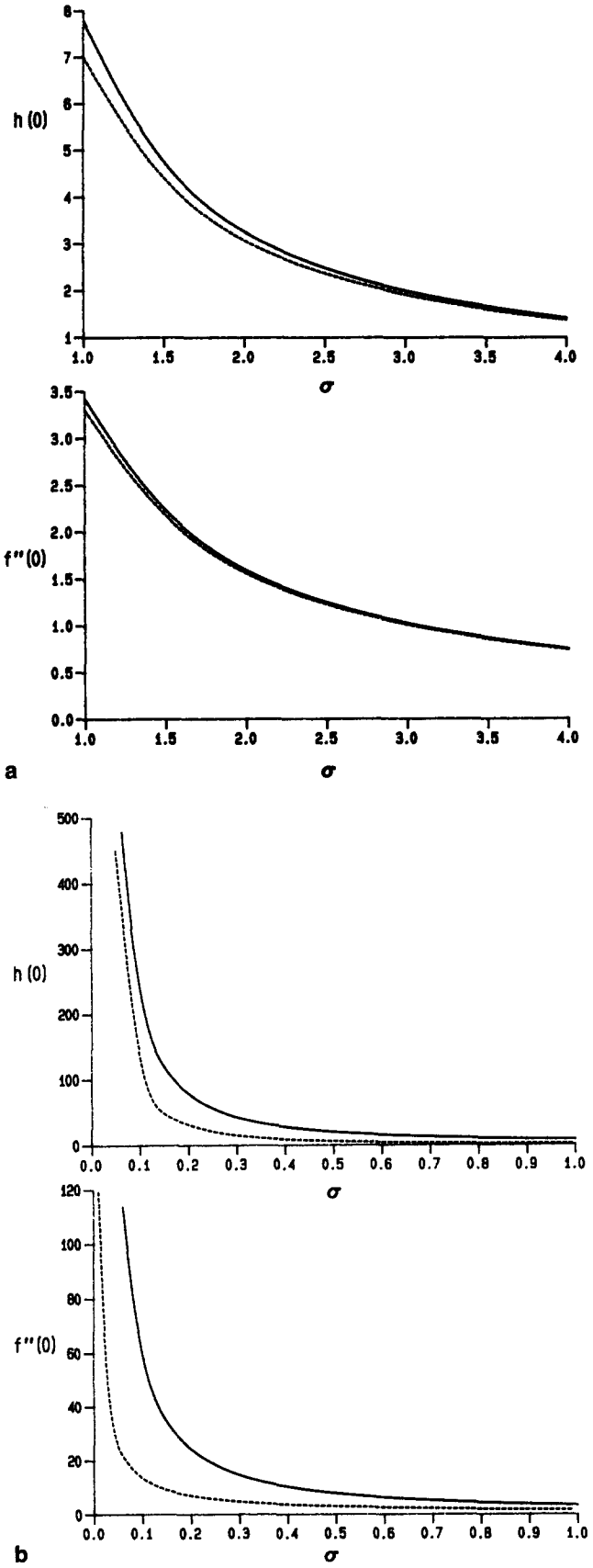

Figure 4 Graphs of $f'(0)$ and $h(0)$ obtained from the numerical integration of Equations 12 for (a) $\sigma \geq 1$ (b) $\sigma \leq 1$. Asymptotic forms (Expressions 37 for $\sigma \gg 1$ and Expressions 51 for $\sigma \ll 1$) are shown by the broken lines

The numerical solution of Equations 25 gives $\phi_0''(0) = 2.5592$, $g_0(0) = 3.8408$, and

$$\phi_0 \sim a_0 y + b_0 \tag{26}$$

where $a_0 = 1.3714$, $b_0 = -0.6322$.

The form of Expression 26 suggests that in the outer region $h \equiv 0$ and that the transformation

$$f = \sigma^{-1/2}\Phi, \quad Y = \sigma^{-1/2} y \tag{27}$$

should be applied, with the outer region having a thickness of $O(\sigma^{1/2})$. On matching with the inner region, it is found that

$$\Phi \sim a_0 Y + \sigma^{-1/2} b_0 + \cdots \quad \text{as } Y \to 0 \tag{28}$$

which suggests that a solution should be sought by expanding

$$\Phi(Y; \sigma) = \Phi_0(Y) + \sigma^{-1/2}\Phi_1(Y) + \cdots \tag{29}$$

At leading order

$$\Phi_0''' + \Phi_0\Phi_0'' - \Phi_0'^2 = 0 \tag{30a}$$

subject to, from Expression 28,

$$\Phi_0 \sim a_0 Y + \cdots \quad \text{as } Y \to 0,\ \Phi_0' \to 0 \quad \text{as } Y \to \infty \tag{30b}$$

The required solution is

$$\Phi_0 = \sqrt{a_0}\,(1 - \exp(-\sqrt{a_0}\,Y)) \tag{31}$$

The equation for the term of $O(\sigma^{-1/2})$ in Expansion 29 is

$$\Phi_1''' + \Phi_0\Phi_1'' - 2\Phi_0'\Phi_1' + \Phi_0''\Phi_1 = 0 \tag{32a}$$

subject to, from Expression 26,

$$\Phi_1 \to b_0 \text{ as } Y \to 0,\ \Phi_1' \to 0 \text{ as } Y \to \infty \tag{32b}$$

The solution is readily obtained as

$$\Phi_1 = b_0 \exp(-\sqrt{a_0}\,Y) \tag{33}$$

Note that Equation 33 makes no contribution to $f(\infty)$, which from Equations 26 and 31 has

$$f(\infty) \sim \sigma^{-1/2}\sqrt{a_0}(1 + O(\sigma^{-1})) \tag{34}$$

The form of the solution in the outer region requires a modification of the solution in the inner region by looking for a solution as an expansion in powers of $\sigma^{-1/2}$, i.e., to put

$$\phi(y; \sigma) = \phi_0(y) + \sigma^{-1/2}\phi_1(y) + \cdots \tag{35}$$
$$g(y; \sigma) = g_0(y) + \sigma^{-1/2} g_1(y) + \cdots$$

The leading-order terms are as before: at $O(\sigma^{-1/2})$, with

$$\phi_1''' + g_1 = 0 \tag{36a}$$

$$g_1'' + \phi_0 g_1' + \phi_1 g_0' - \phi_0' g_1 - \phi_1' g_0 = 0 \tag{36b}$$

subject to

$$\phi_1(0) = 0,\ \phi_1'(0) = 0,\ g_1'(0) = -g_1(0) \tag{36c}$$

on matching with the outer region,

$$\phi_1 \sim b_0 a_0^{1/2} y - \frac{a_0^{3/2}}{2} y^2 + \cdots,\ g_1 \to 0 \qquad \text{as } y \to \infty \tag{36d}$$

The numerical solution of Equations 36 is straightforward.

Finally,

$$\begin{aligned} h(0) &\sim \sigma^{-1}(3.8408 + 3.3355\sigma^{-1/2} + \cdots) \\ f''(0) &\sim \sigma^{-1}(2.5592 + 0.8254\sigma^{-1/2} + \cdots) \end{aligned} \tag{37}$$

as $\sigma \to \infty$. Graphs of $h(0)$ and $f''(0)$ as given by Expressions 37 are also shown in Figure 4a (by the broken lines), and these can be seen to be in very good agreement with the values obtained

from the numerical solution, even at quite moderate values of σ. Expressions 37 also show that both $f''(0)$ and $h(0)$ decrease rapidly as σ is increased.

4.2. Solution for $\sigma \ll 1$

The solution of Equations 12 also develops a two-region structure when σ is small. There is now a relatively thin inner region in which h takes a large and almost constant value and a much thicker outer region at the outer edge of which the outer boundary conditions are obtained.

The discussion starts with the inner region by applying the transformation

$$f = \sigma^{-1/2} w, \quad h = \sigma^{-2} p, \quad \eta = \sigma^{-1/2} y \tag{38}$$

with the inner region being relatively thin, i.e., having a thickness of $O(\sigma^{1/2})$. When transformation 38 is applied to Equations 12, the resulting system is

$$w''' + p + ww'' - w'^2 = 0 \tag{39a}$$

$$p'' + \sigma(wp' - w'p) = 0 \tag{39b}$$

subject to the boundary conditions

$$w(0) = 0, \quad w'(0) = 0, \quad p'(0) = -\sigma^{1/2} p(0) \tag{39c}$$

with the outer boundary conditions relaxed at this stage (primes now denote differentiation with respect to η). The boundary conditions in Equations 39c suggest looking for a solution by expanding

$$w(\eta; \sigma) = w_0(\eta) + \sigma^{1/2} w_1(\eta) + \cdots \tag{40}$$

$$p(\eta; \sigma) = p_0(\eta) + \sigma^{1/2} p_1(\eta) + \cdots$$

At leading order,

$$p_0 = A_0 \tag{41a}$$

for some positive constant A_0 to be determined; then

$$w_0''' + A_0 + w_0 w_0'' - w_0'^2 = 0 \tag{41b}$$

to be solved subject to Equations 39c, and

$$w_0'' \to 0 \quad \text{as} \quad \eta \to \infty \tag{41c}$$

Condition 41c then implies that

$$w_0 \sim \sqrt{A_0}\eta + B_0 \tag{41d}$$

as $\eta \to \infty$ for some further constant B_0. The substitution

$$w_0 = A_0^{1/4} \bar{w}_0, \quad \bar{\eta} = A_0^{1/4} \eta \tag{42}$$

reduces Equation 41b to a standard Falkner–Skan problem, from which it follows that $w_0''(0) = 1.23259\, A_0^{3/4}$ and $B_0 = -0.64790\, A_0^{1/4}$ (Rosenhead 1963).

At $O(\sigma^{1/2})$, on satisfying $p_1'(0) = -A_0$,

$$p_1 = -A_0 \eta + A_1 \tag{43}$$

for some constant A_1. The equation for w_1 then becomes, on applying Equations 42,

$$w_1''' + A_1 A_0^{-3/4} - \bar{\eta} + \bar{w}_0 w_1'' - 2\bar{w}_0' \bar{w}_1' + \bar{w}_0'' w_1 = 0 \tag{44a}$$

Equation 44 has to be solved subject to

$$w_1 \sim -\frac{\bar{\eta}^2}{2} + \tfrac{1}{2}(A_1 A_0^{-3/4} - B_0 A_0^{-1/4})\bar{\eta} + B_1 \quad \text{as } \bar{\eta} \to \infty \tag{44b}$$

A consideration of Expressions 41a, 41d, 43a, and 44b suggests writing for the outer region

$$f = \sigma^{-1} W, \quad h = \sigma^{-2} P \tag{45}$$

and leaving y unscaled. Equations 12 now become

$$P + WW'' - W'^2 + \sigma W''' = 0 \tag{46a}$$

$$P'' + WP' - W'P = 0 \tag{46b}$$

subject to

$$W' \to 0, \; P \to 0 \quad \text{as } y \to \infty \tag{46c}$$

On matching with the inner region,

$$P \sim A_0 - A_0 y + \cdots + \sigma^{1/2}(A_1 + \cdots) + \cdots \tag{46d}$$

$$W \sim \sqrt{A_0}\, y - \sqrt{\frac{A_0}{2}}\, y^2 + \cdots$$

$$+ \sigma^{1/2}(B_0 + \tfrac{1}{2}(A_0^{-1/2} A_1 - B_0) y + \cdots) + \cdots$$

as $y \to 0$.

The above matching conditions (Expressions 46d) suggest looking for a solution by expanding

$$P(y; \sigma) = P_0(y) + \sigma^{1/2} P_1(y) + \cdots \tag{47}$$

$$W(y; \sigma) = W_0(y) + \sigma^{1/2} W_1(y) + \cdots$$

At leading order,

$$P_0 + W_0 W_0'' - W_0'^2 = 0 \tag{48a}$$

$$P_0'' + W_0 P_0' - W_0' P_0 = 0 \tag{48b}$$

The solution of Equations 48 that satisfies both Expressions 46c and the appropriate matching condition from Expressions 46d is

$$A_0 = 1, \; W_0 = 1 - e^{-y}, \; P_0 = e^{-y} \tag{49}$$

The equations at $O(\sigma^{1/2})$ are straightforward to write down, and can also be solved simply. Their solution, using Equations 49, is

$$A_1 = -B_0, \; W_1 = B_0 e^{-y}, \; P_1 = -B_0 e^{-y} \tag{50}$$

Having determined A_0 and A_1, the solution of Equation 44 in the inner region can now be completed, where it is found that $w_1''(0) = 0.41392$, on solving this equation numerically.

Finally, from Equations 38, 49, and 50,

$$h(0) \sim \sigma^{-2}(1 + 0.6479\, \sigma^{1/2} + O(\sigma)) \tag{51}$$

$$f''(0) \sim \sigma^{-3/2}(1.2326 + 0.4139\, \sigma^{1/2} + o(\sigma))$$

as $\sigma \to 0$. Graphs of the asymptotic forms (Expressions 51) are also shown in Figure 4b (by the broken lines). The agreement between Expressions 51 and the numerical solutions is not as good as it is for the case of large Prandtl numbers, being less satisfactory for $f''(0)$ than for $h(0)$. The relatively large discrepancy between the two curves for $f''(0)$ suggests that the contribution to this expression from the $O(\sigma)$ term could well be quite large.

Expressions 51 show that $h(0)$ depends on σ through a relatively large inverse power; $h(0)$ is $O(\sigma^{-2})$ for σ small. This explains why the surface temperature is sensitive to small changes in Prandtl number, with this sensitivity increasing as the Prandtl number is reduced. It is interesting to compare this dependence with that for the prescribed heat-flux problem (Merkin 1989) where the surface temperature was found to be much less sensitive to Prandtl number variations, being on the order of $O(\sigma^{-2/5})$ for σ small. An even more striking difference to Prandtl-number dependence is seen when the present problem is compared with the isothermal surface solution for small Prandtl number (Kuiken 1969). For this problem, the surface heat flux decreases as the Prandtl number decreases, being on the order of $O(\sigma^{1/2})$ for small σ, whereas in the present case the surface heat flux increases rapidly as the Prandtl number decreases, being on the order of $O(\sigma^{-2})$ from Equations 38, 41a, and 43.

Table 1 Comparison between the solution of Equations 12a and 12b with the present boundary conditions, $h'(0) + h(0) = 0$, with prescribed surface temperature, $h(0) = 1$, and with prescribed surface heat flux, $h'(0) = -1$.

	σ	$f''(0)$	$-h'(0)$ or $h(0)$	$f(\infty)$
Newtonian heating	0.72	5.1405	12.3760	2.2201
$h'(0) + h(0) = 0$	7.0	0.4127	0.7430	0.4995
Prescribed temperature	0.72	0.7791	0.5332	1.1836
$h(0) = 1$	7.0	0.5157	1.0771	0.5380
Prescribed heat flux	0.72	1.1362	1.6539	1.3423
$h'(0) = -1$	7.0	0.4932	0.9423	0.5300

5. Discussion

The similarity system given by Equations 12a and 12b and boundary conditions 12c has been considered in some detail. Equations 12a and 12b also arise as free-convection similarity equations when the more usual prescribed surface temperature or prescribed surface heat-flux boundary conditions are applied. In this case, these arise when the surface temperature or heat flux is proportional to x or the distance from the leading edge (Gebhart et al. 1988). It is of interest to compare the solution in the present case, where the surface heat flux and temperature are related via $h'(0) = -h(0)$, with the solution when the surface temperature is prescribed, i.e., with $h(0) = 1$, and with the solution when the surface heat flux is prescribed, i.e., with $h'(0) = -1$. The results are summarized in Table 1 where values of $f''(0)$, $h(0)$ or $-h'(0)$ (as appropriate), and $f(\infty)$ for Prandtl numbers $\sigma = 0.72$ (for air) and $\sigma = 7.0$ (for water at room temperature) are given.

As expected, there are differences in each case in $f''(0)$, $h(0)$ or $-h'(0)$, and $f(\infty)$ between the two values of σ, with these differences being much more marked for the Newtonian-heating case than for the prescribed-temperature and heat-flux cases. This finding is in line with the previous conclusion that the present solution is much more Prandtl-number sensitive (at least for moderate values of σ). Also, the values for $\sigma = 0.72$ for the Newtonian-heating case are substantially higher than the corresponding values for the other two cases. However, for larger values of the Prandtl number ($\sigma = 7.0$), the values $f''(0)$ $-h'(0)$ or $h(0)$, and $f(\infty)$ are comparable in all three cases.

References

Fathalah, K. A. amd Elsayed, M. M. 1980. Natural convection due to solar radiation over a non-absorbing plate with and without heat losses. *Int. J. Heat Fluid Flow*, **2**, 41–45

Gebhart, B., Jaluria, Y., Mahajan, R. L., and Sammakia, B. 1988. *Buoyancy-Induced Flows and Transport*. Hemisphere, New York

Hunt, R. and Wilks, G. 1981. Continuous transformation computation of boundary layer equations between similarity regimes. *J. Comput. Phys.*, **40**, 478–490

Kuiken, H. K. 1969. Free convection at low Prandtl numbers. *J. Fluid Mech.*, **37**, 785–798

Mahmood, T. and Merkin, J. H. 1988. Mixed convection on a vertical cylinder. *J. Applied Math Phys. (ZAMP)*, **39**, 186–203

Merkin, J. H. 1989. Free convection on a heated vertical plate: the solution for small Prandtl number. *J. Eng. Math.*, **23**, 273–282

Merkin, J. H. and Chaudhary, M. A. Submitted. Free convection boundary layers on vertical surfaces driven by an exothermic surface reaction: approximate kinetics

Merkin, J. H. and Pop, I. Submitted. Conjugate free convection on a vertical surface

Pop, I., Sunada, J. K., Cheng, P., and Minkowycz, W. J. 1985. Conjugate free convection from long vertical plate fins embedded in a porous medium. *Int. J. Heat Mass Transfer*, **28**, 1629–1636

Pozzi, A. and Lupo, M. 1988. The coupling of conduction with laminar natural convection along a flat plate. *Int. J. Heat Mass Transfer*, **31**, 1807–1814

Rosenhead, L. (ed.). 1963. *Laminar Boundary Layers*. Clarendon Press, Oxford

Sparrow, E. M. and Gregg, J. L. 1956. Laminar free convection from a vertical plate with uniform surface heat flux. *Trans. ASME*, **78**, 435–440

Stewartson, K. 1957. On asymptotic expansions in the theory of boundary layers. *J. Math. Phys.*, **36**, 173–191

Stewartson, K. 1964. The theory of laminar boundary layers in compressible fluids. Oxford Mathematical Monograph, Oxford University Press